

Inclusive χ_c and b -Quark Production in $\bar{p}p$ Collisions at $\sqrt{s} = 1.8$ TeV

F. Abe,¹² M. Albrow,⁶ D. Amidei,¹⁵ C. Anway-Wiese,² G. Apollinari,²³ M. Atac,⁶ P. Auchincloss,²² P. Azzi,¹⁷ N. Bacchetta,¹⁶ A. R. Baden,⁸ W. Badgett,¹⁵ M. W. Bailey,²¹ A. Bamberger,^{6,*} P. de Barbaro,²² A. Barbaro-Galtieri,¹³ V. E. Barnes,²¹ B. A. Barnett,¹¹ G. Bauer,¹⁴ T. Baumann,⁸ F. Bedeschi,²⁰ S. Behrends,² S. Belforte,²⁰ G. Bellettini,²⁰ J. Bellinger,²⁸ D. Benjamin,²⁷ J. Benlloch,¹⁴ J. Bensinger,² A. Beretvas,⁶ J. P. Berge,⁶ S. Bertolucci,⁷ K. Biery,¹⁰ S. Bhadra,⁹ M. Binkley,⁶ D. Bisello,¹⁷ R. Blair,¹ C. Blocker,² A. Bodek,²² V. Bolognesi,²⁰ A. W. Booth,⁶ C. Boswell,¹¹ G. Brandenburg,⁸ D. Brown,⁸ E. Buckley-Geer,⁶ H. S. Budd,²² G. Busetto,¹⁷ A. Byon-Wagner,⁶ K. L. Byrum,¹ C. Campagnari,⁶ M. Campbell,¹⁵ A. Caner,⁶ R. Carey,⁸ W. Carithers,¹³ D. Carlsmith,²⁸ J. T. Carroll,⁶ R. Cashmore,^{6,*} A. Castro,¹⁷ Y. Cen,¹⁸ F. Cervelli,²⁰ K. Chadwick,⁶ J. Chapman,¹⁵ G. Chiarelli,⁷ W. Chinowsky,¹³ S. Cihangir,⁶ A. G. Clark,⁶ M. Cobal,²⁰ D. Connor,¹⁸ M. Contreras,⁴ J. Cooper,⁶ M. Cordelli,⁷ D. Crane,⁶ J. D. Cunningham,² C. Day,⁶ F. DeJongh,⁶ S. Dell'Agnello,²⁰ M. Dell'Orso,²⁰ L. Demortier,²³ B. Denby,⁶ P. F. Derwent,¹⁵ T. Devlin,²⁴ M. Dickson,²² R. B. Drucker,¹³ A. Dunn,¹⁵ K. Einsweiler,¹³ J. E. Elias,⁶ R. Ely,¹³ S. Eno,⁴ S. Errede,⁹ A. Etchegoyen,^{6,*} B. Farhat,¹⁴ M. Frautschi,¹⁶ G. J. Feldman,⁸ B. Flaugher,⁶ G. W. Foster,⁶ M. Franklin,⁸ J. Freeman,⁶ H. Frisch,⁴ T. Fuess,⁶ Y. Fukui,¹² A. F. Garfinkel,²¹ A. Gauthier,⁹ S. Geer,⁶ D. W. Gerdes,¹⁵ P. Giannetti,²⁰ N. Giokaris,²³ P. Giromini,⁷ L. Gladney,¹⁸ M. Gold,¹⁶ J. Gonzalez,¹⁸ K. Goulianos,²³ H. Grassmann,¹⁷ G. M. Grieco,²⁰ R. Grindley,¹⁰ C. Grosso-Pilcher,⁴ C. Haber,¹³ S. R. Hahn,⁶ R. Handler,²⁸ K. Hara,²⁶ B. Harral,¹⁸ R. M. Harris,⁶ S. A. Hauger,⁵ J. Hauser,³ C. Hawk,²⁴ T. Hessing,²⁵ R. Hollebeek,¹⁸ L. Holloway,⁹ A. Hölischer,¹⁰ S. Hong,¹⁵ G. Houk,¹⁸ P. Hu,¹⁹ B. Hubbard,¹³ B. T. Huffman,¹⁹ R. Hughes,²² P. Hurst,⁸ J. Huth,⁶ J. Hysten,⁶ M. Incagli,²⁰ T. Ino,²⁶ H. Iso,²⁶ H. Jensen,⁶ C. P. Jessop,⁸ R. P. Johnson,⁶ U. Joshi,⁶ R. W. Kadel,¹³ T. Kamon,²⁵ S. Kanda,²⁶ D. A. Kardelis,⁹ I. Karliner,⁹ E. Kearns,⁸ L. Keeble,²⁵ R. Kephart,⁶ P. Kesten,² R. M. Keup,⁹ H. Keutelian,⁶ D. Kim,⁶ S. B. Kim,¹⁵ S. H. Kim,²⁶ Y. K. Kim,¹³ L. Kirsch,² K. Kondo,²⁶ J. Konigsberg,⁸ K. Kordas,¹⁰ E. Kovacs,⁶ M. Krasberg,¹⁵ S. E. Kuhlmann,¹ E. Kuns,²⁴ A. T. Laasanen,²¹ S. Lammel,³ J. I. Lamoureux,²⁸ S. Leone,²⁰ J. D. Lewis,⁶ W. Li,¹ P. Limon,⁶ M. Lindgren,³ T. M. Liss,⁹ N. Lockyer,¹⁸ M. Loretto,¹⁷ E. H. Low,¹⁸ D. Lucchesi,²⁰ C. B. Luchini,⁹ P. Lukens,⁶ P. Maas,²⁸ K. Maeshima,⁶ M. Mangano,²⁰ J. P. Marriner,⁶ M. Mariotti,²⁰ R. Markeloff,²⁸ L. A. Markosky,²⁸ J. A. J. Matthews,¹⁶ R. Mattingly,² P. McIntyre,²⁵ A. Menzione,²⁰ E. Meschi,²⁰ T. Meyer,²⁵ S. Mikamo,¹² M. Miller,⁴ T. Mimashi,²⁶ S. Miscetti,⁷ M. Mishina,¹² S. Miyashita,²⁶ Y. Morita,²⁶ S. Moulding,²³ J. Mueller,²⁴ A. Mukherjee,⁶ T. Muller,³ L. F. Nakae,² I. Nakano,²⁶ C. Nelson,⁶ D. Neuberger,³ C. Newman-Holmes,⁶ J. S. T. Ng,⁸ M. Ninomiya,²⁶ L. Nodulman,¹ S. Ogawa,²⁶ R. Paoletti,²⁰ V. Papadimitriou,⁶ A. Para,⁶ E. Pare,⁸ S. Park,⁶ J. Patrick,⁶ G. Pauletta,²⁰ L. Pescara,¹⁷ T. J. Phillips,⁵ A. G. Piacentino,²⁰ R. Plunkett,⁶ L. Pondrom,²⁸ J. Proudfoot,¹ F. Ptohos,⁸ G. Punzi,²⁰ D. Quarrie,⁶ K. Ragan,¹⁰ G. Redlinger,⁴ J. Rhoades,²⁸ M. Roach,²⁷ F. Rimondi,^{6,*} L. Ristori,²⁰ W. J. Robertson,⁵ T. Rodrigo,⁶ T. Rohaly,¹⁸ A. Roodman,⁴ W. K. Sakumoto,²² A. Sansoni,⁷ R. D. Sard,⁹ A. Savoy-Navarro,⁶ V. Scarpine,⁹ P. Schlabach,⁸ E. E. Schmidt,⁶ O. Schneider,¹³ M. H. Schub,²¹ R. Schwitters,⁸ G. Sciaccia,²⁰ A. Scribano,²⁰ S. Segler,⁶ S. Seidel,¹⁶ Y. Seiya,²⁶ G. Sganos,¹⁰ M. Shapiro,¹³ N. M. Shaw,²¹ M. Sheaff,²⁸ M. Shochet,⁴ J. Siegrist,¹³ A. Sill,²² P. Sinervo,¹⁰ J. Skarha,¹¹ K. Sliwa,²⁷ D. A. Smith,²⁰ F. D. Snider,¹¹ L. Song,⁶ T. Song,¹⁵ M. Spahn,¹³ P. Sphicas,¹⁴ A. Spies,¹¹ R. St. Denis,⁸ L. Stanco,¹⁷ A. Stefanini,²⁰ G. Sullivan,⁴ K. Sumorok,¹⁴ R. L. Swartz, Jr.,⁹ M. Takano,²⁶ K. Takikawa,²⁶ S. Tarem,² F. Tartarelli,²⁰ S. Tether,¹⁴ D. Theriot,⁶ M. Timko,²⁶ P. Tipton,²² S. Tkaczyk,⁶ A. Tollestrup,⁶ J. Tonnison,²¹ W. Trischuk,⁸ Y. Tsay,⁴ J. Tseng,¹¹ N. Turini,²⁰ F. Ukegawa,²⁶ D. Underwood,¹ S. Vejck III,¹⁵ R. Vidal,⁶ R. G. Wagner,¹ R. L. Wagner,⁶ N. Wainer,⁶ R. C. Walker,²² J. Walsh,¹⁸ A. Warburton,¹⁰ G. Watts,²² T. Watts,²⁴ R. Webb,²⁵ C. Wendt,²⁸ H. Wenzel,²⁰ W. C. Wester III,¹³ T. Westhusing,⁹ S. N. White,²³ A. B. Wicklund,¹ E. Wicklund,⁶ H. H. Williams,¹⁸ B. L. Winer,²² J. Wolinski,²⁵ D. Y. Wu,¹⁵ X. Wu,²⁰ J. Wyss,¹⁷ A. Yagil,⁶ W. Yao,¹³ K. Yasuoka,²⁶ Y. Ye,¹⁰ G. P. Yeh,⁶ J. Yoh,⁶ M. Yokoyama,²⁶ J. C. Yun,⁶ A. Zanetti,²⁰ F. Zetti,²⁰ S. Zhang,¹⁵ W. Zhang,¹⁸ and S. Zucchelli^{6,*}

(CDF Collaboration)

¹Argonne National Laboratory, Argonne, Illinois 60439

²Brandeis University, Waltham, Massachusetts 02254

³University of California at Los Angeles, Los Angeles, California 90024

- ⁴University of Chicago, Chicago, Illinois 60637
⁵Duke University, Durham, North Carolina 27706
⁶Fermi National Accelerator Laboratory, Batavia, Illinois 60510
⁷Laboratori Nazionali di Frascati, Istituto Nazionale di Fisica Nucleare, Frascati, Italy
⁸Harvard University, Cambridge, Massachusetts 02138
⁹University of Illinois, Urbana, Illinois 61801
¹⁰Institute of Particle Physics, McGill University, Montreal, and University of Toronto, Toronto, Canada
¹¹The Johns Hopkins University, Baltimore, Maryland 21218
¹²National Laboratory for High Energy Physics (KEK), Tsukuba, Ibaraki 305, Japan
¹³Lawrence Berkeley Laboratory, Berkeley, California 94720
¹⁴Massachusetts Institute of Technology, Cambridge, Massachusetts 02139
¹⁵University of Michigan, Ann Arbor, Michigan 48109
¹⁶University of New Mexico, Albuquerque, New Mexico 87131
¹⁷Università di Padova, Istituto Nazionale di Fisica Nucleare, Sezione di Padova, I-35131 Padova, Italy
¹⁸University of Pennsylvania, Philadelphia, Pennsylvania 19104
¹⁹University of Pittsburgh, Pittsburgh, Pennsylvania 15260
²⁰Istituto Nazionale di Fisica Nucleare, University and Scuola Normale Superiore of Pisa, I-56100 Pisa, Italy
²¹Purdue University, West Lafayette, Indiana 47907
²²University of Rochester, Rochester, New York 15627
²³Rockefeller University, New York, New York 10021
²⁴Rutgers University, Piscataway, New Jersey 08854
²⁵Texas A&M University, College Station, Texas 77843
²⁶University of Tsukuba, Tsukuba, Ibaraki 305, Japan
²⁷Tufts University, Medford, Massachusetts 02155
²⁸University of Wisconsin, Madison, Wisconsin 53706
(Received 21 May 1993)

We report the full reconstruction of χ_c mesons through the decay chain $\chi_c \rightarrow J/\psi \gamma$, $J/\psi \rightarrow \mu^+ \mu^-$, using data obtained at the Collider Detector at Fermilab in $2.6 \pm 0.2 \text{ pb}^{-1}$ of $\bar{p}p$ collisions at $\sqrt{s} = 1.8 \text{ TeV}$. This exclusive χ_c sample is used to measure the χ_c -meson production cross section times branching fractions. We obtain $\sigma \times B = 3.2 \pm 0.4(\text{stat}) \pm 1.7(\text{syst}) \text{ nb}$ for χ_c mesons decaying to J/ψ with $p_T > 6.0 \text{ GeV}/c$ and pseudorapidity $|\eta| < 0.5$. From this and the inclusive J/ψ cross section we calculate the inclusive b -quark cross section to be $12.0 \pm 4.5 \mu\text{b}$ for $p_T^b > 8.5 \text{ GeV}/c$ and $|y^b| < 1$.

PACS numbers: 13.85.Ni, 14.40.Gx, 14.80.Dq

This Letter reports the full reconstruction of χ_c mesons in $\sqrt{s} = 1.8 \text{ TeV}$ $\bar{p}p$ collisions, through the decay chain $\chi_c \rightarrow J/\psi \gamma$, $J/\psi \rightarrow \mu^+ \mu^-$. The observed χ_c sample is used to measure the χ_c production cross section times branching fractions for the unresolved χ_c angular momentum states. Although χ_c production has been observed at a lower energy hadron collider [1] in the same decay channel, our results, based upon data observed at the Collider Detector at Fermilab (CDF), are the first obtained at Tevatron energies.

Two mechanisms have been proposed for the production of charmonium states at Tevatron energies: direct charmonium production and the decay of b -flavored hadrons [2,3]. The latter mechanism is predicted to dominate production of high-transverse-momentum (p_T) J/ψ mesons, with χ_c decays contributing more than 90% of the remaining "direct" J/ψ production rate. In contrast, χ_c -meson production is expected to proceed largely through direct gluon fusion [3–6], and should dominate production via b -hadron decay by about 4:1. A measurement of the χ_c production cross section therefore provides a test of direct charmonium production models. In addition, the χ_c cross section can be used in combination with the inclusive J/ψ production cross section measured in a

previous publication by CDF [7] to calculate the b -quark cross section under the assumption that direct J/ψ production contributes negligibly to the total J/ψ rate.

The CDF has been described in detail elsewhere [8]. The events in this analysis were collected using a multilevel muon trigger system. The level-one trigger required the presence of a charged track in the muon chambers (covering pseudorapidity $|\eta| < 0.65$) with a transverse momentum (p_T) above a nominal threshold of $3 \text{ GeV}/c$. The level-two trigger required two muon chamber tracks which matched charged tracks in the central tracking chamber (CTC), with a separation of at least one muon chamber (15° wide in azimuth) between the two muon candidates. We collected an integrated luminosity of $2.6 \pm 0.2 \text{ pb}^{-1}$ using this trigger.

The trigger efficiency for each muon was the product of the level-one and level-two efficiencies. The efficiencies for the two muons were uncorrelated by virtue of their geometrical separation. The level-one and level-two efficiencies have been studied using muon candidates in data taken with no muon-specific trigger requirements. The level-one trigger efficiency increased with muon p_T from $(44 \pm 4)\%$ at $p_T = 2.0 \text{ GeV}/c$ to $(92 \pm 4)\%$ for $p_T > 6.0 \text{ GeV}/c$. The level-two trigger efficiency rose

sharply from $(10 \pm 5)\%$ at $p_T = 2.0$ GeV/c to $(99 \pm 1)\%$ for $p_T > 3.0$ GeV/c.

Transverse momenta were calculated from track curvatures in the 1.41 T axial magnetic field. Constraining the tracks to the primary vertex yielded a momentum resolution of $\delta p_T/p_T = \sqrt{(0.0011 p_T)^2 + (0.0066)^2}$ where p_T was in GeV/c. To check the momentum scale, we reconstructed the following decays: $J/\psi \rightarrow \mu^+ \mu^-$, $\psi(2S) \rightarrow \mu^+ \mu^-$, $\Upsilon(1S) \rightarrow \mu^+ \mu^-$, $\Upsilon(2S) \rightarrow \mu^+ \mu^-$, and $\Upsilon(3S) \rightarrow \mu^+ \mu^-$. After corrections for dE/dx losses, we obtained the mass values 3.097 ± 0.001 , 3.687 ± 0.007 , 9.458 ± 0.004 , 10.02 ± 0.01 , and 10.36 ± 0.01 GeV/c², respectively, in agreement with world average values [9].

To reconstruct χ_c mesons, we first identified J/ψ mesons by requiring two oppositely charged muon candidates, each with $p_T > 3.0$ GeV/c. For each muon, we calculated the difference in both the transverse and longitudinal directions between the position of the muon chamber track and the CTC track extrapolated to the muon chamber position. Requiring these differences to be less than 3 times the uncertainty expected from measurement errors, energy loss, and multiple scattering removed approximately 50% of the background to the $\mu^+ \mu^-$ signal from punchthrough and decay-in-flight, while being $(97 \pm 2)\%$ efficient for keeping real muon pairs. Finally, we selected muon pairs with $p_T > 6.0$ GeV/c and $|\eta| < 0.5$. The resulting $\mu^+ \mu^-$ mass distribution is shown in Fig. 1, along with a fit to a Gaussian plus a constant background. The width of the Gaussian is $\sigma = 0.018$ GeV/c². Defining our J/ψ sample as those events with dimuon mass between 3.05 and 3.15 GeV/c², we observed 896 ± 32 reconstructed J/ψ events above a background of 45 ± 8 .

Photon candidates were then selected by demanding an

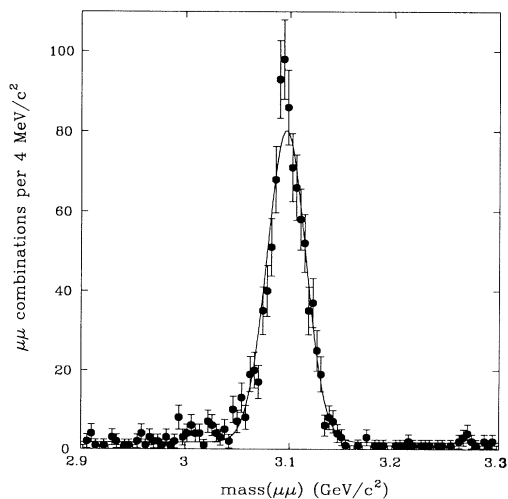


FIG. 1. The mass distribution of $\mu^+ \mu^-$ for the J/ψ mass region. The data are shown as points and the solid curve is a fit to a Gaussian plus a constant background.

electromagnetic energy deposition with at least 1 GeV in $|\eta| < 0.7$ and a cluster in the electromagnetic strip chambers. These chambers were located at a depth of six radiation lengths in the calorimeter. The energy resolution was $\sigma(E) \approx 18\% \sqrt{E}$ (E in GeV) for energies below 5 GeV. We rejected photon candidates that occurred in any calorimeter tower traversed by one of the muons. The photon direction was determined from the position of the strip chamber cluster and, by assumption, the muon pair vertex. The position resolution at the strip chamber was ≈ 1 cm. The energy and direction of the photon candidate were combined with the muon momenta to determine the invariant mass of the $\mu^+ \mu^- \gamma$ system. The mass difference $[\Delta M = M(\mu^+ \mu^- \gamma) - M(\mu^+ \mu^-)]$ distribution is shown in Fig. 2. A clear χ_c signal is present near $\Delta M = 0.4$ GeV, but the individual χ_c angular momentum states are not resolved. The ΔM resolution was dominated by the photon energy resolution.

The primary source of background was from J/ψ events in which a photon from a π^0 decay passed the photon identification requirements. The shape of the background ΔM spectrum was determined using real $J/\psi \rightarrow \mu^+ \mu^-$ events containing charged tracks other than muons. The momenta of these tracks were used as input to a Monte Carlo program that generated decays of neutral pions into photons. The ΔM spectrum of the J/ψ and these simulated photons, weighted by the photon finding efficiency, was normalized to the sideband region of the observed spectrum and parametrized. The range of parametrizations consistent with this background shape is also shown in Fig. 2. The central parametrization curve in this figure was used for calculating our signal size.

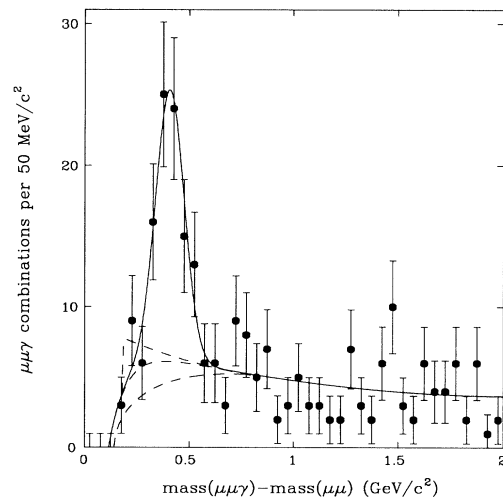


FIG. 2. The mass difference ΔM for the χ_c mass region. The data are shown as points and the solid curve is a fit to a Gaussian plus the background shape as mentioned in the text. The three dashed curves show the range of background parametrizations consistent with the estimated background distribution.

The number of χ_c events was determined using a binned maximum likelihood technique to fit the ΔM distribution to a Gaussian signal plus the independently determined background shape. The fit produced 67 ± 8 (statistical) signal events with a mean mass difference of 0.406 ± 0.013 GeV/ c^2 . This mass difference is consistent with the expectation that the unresolved χ_c signal consists of 90% χ_{c1} ($\Delta M = 0.4136$ GeV/ c^2) and 10% χ_{c2} ($\Delta M = 0.4592$ GeV/ c^2) [5,9]. The width of the Gaussian was 70 ± 12 MeV/ c^2 , as expected from the photon energy resolution. Uncertainty in the background shape contributed an uncertainty of $\pm 9\%$ in the observed number of χ_c mesons.

We determined our χ_c detection efficiency using a Monte Carlo simulation which incorporated the shape of the χ_c p_T and rapidity spectra as given by the theoretical calculations of Humpert [5] and Nason, Dawson, and Ellis [10]. A sample of χ_c decaying to $J/\psi \gamma$ was generated within the kinematic region $6 \leq p_T^{J/\psi} \leq 20$ and $|\eta^{J/\psi}| \leq 0.5$. Additionally, we assumed that $(16 \pm 8)\%$ of the χ_c mesons in this region originated from B meson decays [11], the balance from direct production mechanisms. This assumption was later checked by demanding consistency with the fraction deduced from the observed $B \rightarrow J/\psi X$ cross section [7] and the $B \rightarrow \chi_c X$ and $B \rightarrow J/\psi X$ branching fractions [5,9]. Uncertainty in the p_T and η distributions of the χ_c introduced a 25% uncertainty in the overall χ_c acceptance.

Parametrizations of the level-one and level-two trigger efficiencies as a function of p_T and polar angle were applied to the simulated muons. By varying the parameters within $\pm 1\sigma$ from those measured, we found an associated uncertainty of $\pm 9\%$ in the acceptance.

The muon chamber active area covered 85% of the solid angle in the region $|\eta| < 0.65$. The chamber acceptance was determined by requiring simulated muons with $p_T > 3$ GeV/ c to pass through this muon fiducial volume. The total χ_c acceptance was then obtained by folding in the muon reconstruction efficiency, the photon reconstruction efficiency, and the J/ψ mass window acceptance.

We measured the muon reconstruction efficiency from cosmic ray data. Combining the individual contributions to the efficiency from the CTC track reconstruction [(97 \pm 2)%], muon chamber track reconstruction [(98 \pm 1)%], and track matching criteria [(97 \pm 2)%] yielded an overall muon reconstruction efficiency of (92 \pm 3)% for muons with $p_T > 3$ GeV/ c . The J/ψ mass window requirement was (97 \pm 2)% efficient.

Photon reconstruction efficiencies were measured by examining a sample of electrons from photon conversions in which one of the electrons was selected using only tracking information. We calculated the electron efficiency from the number of electron tracks that passed the calorimeter and strip chamber criteria for photons. A 13% uncertainty arose from limited electron statistics. The resulting electron efficiency was converted to a pho-

TABLE I. Uncertainties in $\sigma(\chi_c \rightarrow \mu^+ \mu^- \gamma)$.

Quantity	Uncertainty
N_{χ_c}	12% (stat), $\pm 19\%$ (syst)
Luminosity, L	$\pm 7.7\%$
Efficiency, ϵ , arising from	$\pm 33\%$
(1) Trigger	$\pm 9\%$
(2) μ identification	$\pm 3\%$
(3) J/ψ mass window	$\pm 2\%$
(4) Photon identification	$\pm 16\%$
(5) χ_c polarization	$\pm 11\%$
(6) χ_c p_T and η distributions	$\pm 25\%$
Uncertainty in $\sigma(\chi_c \rightarrow \mu^+ \mu^- \gamma)$	± 0.4 (stat) ± 1.7 nb

ton efficiency by correcting for the difference in calorimeter response for electrons and photons using a GEANT [12] simulation of the detector. The correction was less than 10% for all photon energies. We estimated an uncertainty of $\pm 9\%$ in the acceptance arising from uncertainties in the electron efficiency measurement and the GEANT simulation. Combining the 13% and 9% uncertainties yielded a total photon efficiency uncertainty of 16%.

The unknown polarization of the χ_c mesons introduced an uncertainty in the acceptance calculation. We determined this uncertainty to be $\pm 11\%$ by varying the polarization of the χ_c in the Monte Carlo simulation over the entire allowed range.

The combined detection efficiency for $\chi_c \rightarrow J/\psi \gamma$ with $J/\psi \rightarrow \mu^+ \mu^-$ was $(0.79 \pm 0.26)\%$ where the uncertainty represents the sum in quadrature of all the systematic uncertainties from the preceding discussion. Table I summarizes the various contributions to the uncertainty in acceptance.

The χ_c cross section times branching fraction was calculated using the formula

$$\sigma(\chi_c \rightarrow \mu^+ \mu^- \gamma) = N_{\chi_c} / \epsilon L, \quad (1)$$

where $\sigma(\chi_c \rightarrow \mu^+ \mu^- \gamma)$ is the cross section for the process $\bar{p}p \rightarrow \chi_c X \rightarrow J/\psi \gamma X \rightarrow \mu^+ \mu^- \gamma X$, N_{χ_c} is the number of observed χ_c events, ϵ is the χ_c detection efficiency, and L is the integrated luminosity. We obtained

$$\sigma(\chi_c \rightarrow \mu^+ \mu^- \gamma) = 3.2 \pm 0.4(\text{stat}) \pm 1.7(\text{syst}) \text{ nb}$$

for χ_c decaying to J/ψ with $p_T > 6.0$ GeV/ c and

TABLE II. Calculation of b -quark cross section.

$B(J/\psi \rightarrow \mu^+ \mu^-) \sigma(\bar{p}p \rightarrow J/\psi X)$	6.88 ± 1.11 nb
$\sigma(\chi_c \rightarrow \mu^+ \mu^- \gamma)$	3.2 ± 1.2 nb
$B(J/\psi \rightarrow \mu^+ \mu^-)$	$5.97 \pm 0.25\%$
$B(B \rightarrow J/\psi X)_{\text{no } \chi_c}$	$1.1 \pm 0.2\%$
R	4.28 ± 0.02
$\sigma^b, p_T^b > 8.5$ GeV/ $c, y < 1$	12.0 ± 4.5 μb

$|\eta| < 0.5$, where the result was summed over the χ_c angular momentum states. The first uncertainty is statistical and the second combines in quadrature the systematic uncertainties due to the fitting procedure, the efficiency calculation, and the luminosity measurement, as summarized in Table I.

By assuming χ_c and B meson decays constituted the total J/ψ production rate (neglecting an expected 1% con-

tribution to the inclusive J/ψ rate from decay of *direct* ψ' [3,7]), we could determine the b -quark cross section from the above result and the inclusive J/ψ cross section [7]. To convert the $B \rightarrow J/\psi$ rate into the b -quark cross section, we multiplied by the ratio R of the b -quark cross section to the observed J/ψ cross section as determined using a Monte Carlo program, a full detector simulation and the same analysis as performed on the data:

$$\sigma^b(p_T^b > p_T^{\min}, |y^b| < 1) = \frac{B(J/\psi \rightarrow \mu^+ \mu^-) \sigma(\bar{p}p \rightarrow J/\psi X) - \sigma(\chi_c \rightarrow \mu^+ \mu^- \gamma)}{2B(B \rightarrow J/\psi X|_{\text{no}\chi_c}) B(J/\psi \rightarrow \mu^+ \mu^-)} R. \quad (2)$$

Here

$$R = \frac{\sigma_{\text{MC}}^b(p_T^b > p_T^{\min}, |y^b| < 1)}{\sigma_{\text{MC}}^{J/\psi}(p_T^{J/\psi} > 6 \text{ GeV}/c, |\eta^{J/\psi}| < 0.5)}, \quad (3)$$

and $B(B \rightarrow J/\psi X|_{\text{no}\chi_c})$ is that part of the B -to- J/ψ decay which does not include χ_c intermediate states. The value of p_T^{\min} was chosen such that approximately 90% of the Monte Carlo J/ψ events originated from b quarks with $p_T^b > p_T^{\min}$. We found $p_T^{\min} = 8.5 \text{ GeV}/c$. The Monte Carlo program generated b quarks according to the p_T and rapidity distributions provided by Nason, Dawson, and Ellis [10], and fragmented the b quark into mesons using the Peterson fragmentation model [13], with $\epsilon_P = 0.006$. The J/ψ momentum spectrum in the B rest frame was taken from ARGUS data [14].

Evaluating Eq. (2) yielded the result $\sigma(b) = 12.0 \pm 4.5 \mu\text{b}$ for $p_T^b > 8.5 \text{ GeV}/c$ and $|y^b| < 1$. The calculation is summarized in Table II. This result is consistent with that obtained from the $\psi(2S)$ inclusive cross section, $10.5 \pm 5 \mu\text{b}$ [7]. The value of $\sigma(b)$ relies on the assumption that direct J/ψ production is negligible. If this assumption is changed to one in which direct production accounts for 9% of the J/ψ mesons then the value for $\sigma(b)$ drops by 6%.

We thank the Fermilab staff and the technical staffs of the participating institutions for their vital contributions. This work was supported by the U.S. Department of Energy and National Science Foundation, the Italian Istituto Nazionale di Fisica Nucleare, the Ministry of Science, Culture, and Education of Japan, the Natural Sciences and Engineering Research Council of Canada, the A.P. Sloan Foundation, and the Alexander von Humboldt Stiftung.

*Visitor.

[1] C. Kourkoumelis *et al.*, Phys. Lett. **81B**, 405 (1979).

[2] M. L. Mangano, INFN Report No. IFUP-TH 2/93, 1993

(to be published).

- [3] E. W. N. Glover, A. D. Martin, and W. J. Stirling, Z. Phys. C **38**, 473 (1988).
- [4] R. Baier and R. Rückl, Nucl. Phys. **B208**, 381 (1982); Z. Phys. C **19**, 251 (1983).
- [5] We performed a similar calculation for J/ψ with the same QCD parameters and K factor as Ref. [3], using the parton-parton differential cross sections of Humpert in the ISAJET program (Ref. [15]), and $Q^2 = (M_\chi^2 + p_T^2)/4$ [16]. Although this calculation does not include the small direct J/ψ production, it yielded a shape for the cross section similar to that of Ref. [3]. B. Humpert, Phys. Lett. **B 184**, 105 (1987); C. Albajar *et al.*, Phys. Lett. **B 256**, 112 (1991).
- [6] R. Gastmans, W. Troost, and Tai Tsun Wu, Phys. Lett. **B 184**, 257 (1987).
- [7] F. Abe *et al.*, Phys. Rev. Lett. **69**, 3704 (1992).
- [8] F. Abe *et al.*, Nucl. Instrum. Methods Phys. Res., Sect. A **271**, 387 (1988); R. Bedeschi *et al.*, Nucl. Instrum. Methods Phys. Res., Sect. A **268**, 50 (1988); G. Ascoli *et al.*, Nucl. Instrum. Methods Phys. Res., Sect. A **268**, 33 (1988).
- [9] Particle Data Group, K. Hikasa *et al.*, Phys. Rev. D **45**, II.18 (1992).
- [10] P. Nason, S. Dawson, and R. K. Ellis, Nucl. Phys. **B303**, 607 (1988); **B327**, 49 (1989); **B335**, 260 (1990). We have used their choice of parameters in the Monte Carlo simulation: $m_B = 4.75 \text{ GeV}/c^2$, $\Lambda_4 = 270 \text{ MeV}$, and the DFLM; $m_B = 4.75 \text{ GeV}/c^2$, $\Lambda_4 = 270 \text{ MeV}$, and the DFLM structure functions.
- [11] B. Gittelmann, in *Proceedings of the Vancouver Meeting (1991 DPF Meeting)* (World Scientific, Singapore, 1991), p. 181.
- [12] R. Brun *et al.*, GEANT3, CERN DD/EE/84-1.
- [13] C. Peterson *et al.*, Phys. Rev. D **27**, 105 (1983).
- [14] H. Schroder (private communication).
- [15] F. Paige and S. D. Protopopescu, ISAJET Monte Carlo version 6.36, BNL Report No. BNL38034, 1986 (unpublished).
- [16] E. W. N. Glover (private communication).